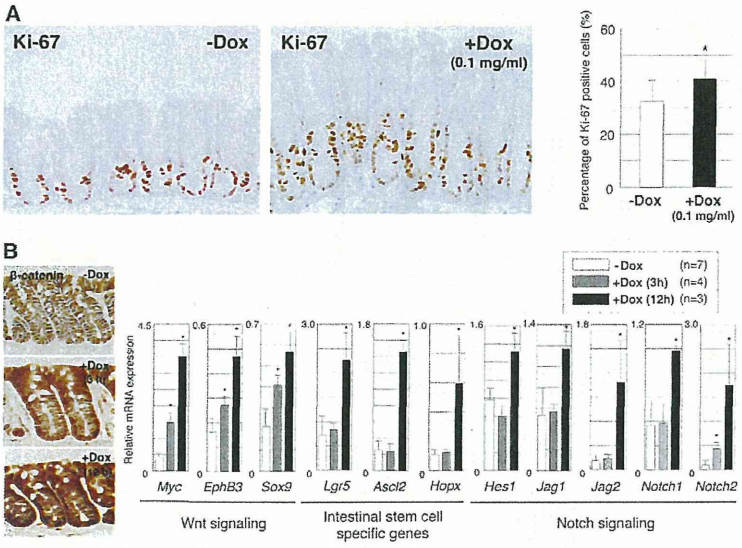

Fig. 5. Dose-dependent effect of Wnt activation on cell proliferation and gene expression in colonic epithelium. (**A**) Lower level of β-catenin induction promotes colonic epithelial proliferation. Ki-67 immunostaining and percentage of Ki-67-positive cells in colonic section from β-catenin-inducible mice treated with lower dose of doxycycline. Lower levels of β-catenin induction increase Ki-67 positive cell ratio and elongate the proliferating compartment of the crypts. Data are mean ± s.d.; **P*<0.05, by Welch's *t*-test. (**B**) Expression of Wnt target genes, ISC-specific genes and Notch signalling-related genes in the colonic crypts with different levels of β-catenin. The different levels of β-catenin accumulation are shown in the left-hand panels. Data are mean ± s.d.; **P*<0.05 compared with non-treated mice, by Kruskal–Wallis test followed by Steel test.

Hes1 in β-catenin-induced mice treated with the Notch inhibitor (data not shown). It is possible that the Notch inhibitor led to a transient inactivation of Notch signalling and thus the altered *Hes1* expression was not detectable at 2 days after treatment. However, given that the Notch/γ-secretase inhibitor has multiple substrates, we cannot completely rule out the possibility that the effect was partly independent of Notch inhibition.

Lower levels of β-catenin activation induce active proliferation of progenitor cells, but not stem cell expansion

In contrast to the well-established role of canonical Wnt signalling in activating cell proliferation in the intestine (Sansom et al., 2004; Andreu et al., 2005), our data show that the Wnt activation confers slow-cycling properties on colonic cells, which is accompanied by *de novo* crypt formation. In an attempt to consolidate these opposing results, we hypothesised that different levels of Wnt signalling may induce different biological outcomes with elevated levels of activation leading to the expansion of slow-cycling ISC-like cells and lower levels of activation inducing active cell proliferation. In order to determine the effects of different levels of β-catenin induction on colon homeostasis, we treated β-catenin-inducible mice with a lower dose of doxycycline than was used previously (0.1 mg/ml in drinking water) and analysed crypt sections. Colonic crypts did not show signs of increased crypt fission/branching rate in mice, suggesting that *de novo* crypt formation is not induced when β-catenin is expressed at low levels (Fig. 5A). However, low levels of β-catenin increased the number of Ki-67-positive cells, and led to an elongation of crypts (Fig. 5A), indicative of enhanced cell proliferation of progenitor cells. These results suggest that different strengths of canonical Wnt signalling result in different transcriptional outputs and, thus, biological effects.

To examine the effects of different levels of Wnt signalling on transcription, we performed gene expression analyses of colonic crypts with high and low levels of β-catenin accumulation. β-Catenin-inducible mice were intragastrically administered doxycycline (100 mg/kg) and sacrificed 3 and 12 hours later, leading to different levels of β-catenin accumulation in the colonic crypts (Fig. 5B). We found that *Myc*, *EphB3* and *Sox9*, well-known targets of canonical Wnt signalling, were upregulated in crypts with both higher and lower levels of β-catenin expression in a level-dependent manner (Fig. 5B). However, activation of the Notch target gene *Hes1* was detected only in crypts with high β-catenin, which is accompanied by the upregulation of ISC-specific genes including *Lgr5*, *Ascl2* and *Hopx* (Fig. 5B). We also examined the gene expression in colonic crypts isolated from β-catenin-inducible mice treated with a lower dose of doxycycline in drinking water (0.1 mg/ml) and found that the lower dose treatment significantly upregulated the expression of Wnt target genes such as *Myc*, but the same treatment did not induce *Lgr5* and *Hes1* in colonic crypts (supplementary material Fig. S9). Together, these results show that activation of the Notch signalling pathway and amplification of ISC-like cells require higher level of β-catenin accumulation. In addition, the expression of the Cdk inhibitors *Cdkn1a*, *Cdkn1b* and *Cdkn1c* were not altered by the lower level of β-catenin induction (supplementary material Fig. S9) in sharp contrast to the case of the higher level of β-catenin induction (supplementary material Fig. S5), suggesting that altered expression of Cdk inhibitors might be responsible for the different proliferative activities.

Colon tumors show heterogeneity in nuclear β-catenin expression and slow-cycling cells in the *Apc*$^{Min/+}$ mouse model

A large body of evidence indicates that accumulation of β-catenin is an initiating event in intestinal carcinogenesis (Harada et al., 1999; Yamada et al., 2002). The vast majority of colon cancers show accumulation of β-catenin and expression of elevated levels of β-catenin/Tcf target genes. However, strong nuclear accumulation of β-catenin is only observed in a subset of tumour cells, indicating heterogeneity of tumour cells within the tumour (Fodde and Brabletz, 2007). Similarly, we found that colon tumours in *Apc*$^{Min/+}$ mice, a well-established model for colon tumorigenesis, also show heterogeneous expression of nuclear β-catenin (Fig. 6A). To determine whether such heterogeneous expression of nuclear β-catenin affects downstream transcription of the canonical Wnt signalling, we examined colon tumours of *Apc*$^{Min/+}$ mice carrying a transgenic GFP reporter allele of β-catenin/Tcf transcription (Oyama et al., 2008). Double

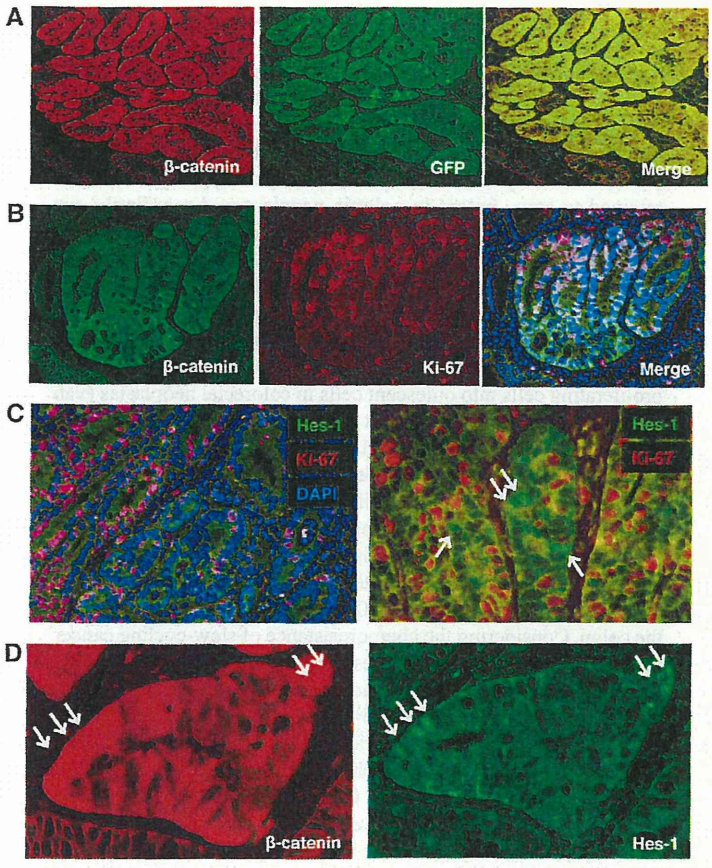

Fig. 6. Heterogeneity of colon tumour cells in $Apc^{Min/+}$ mouse. (**A**) Double immunostaining for β-catenin (red) and GFP (green) in the colon tumour of $Apc^{Min/+}$ mouse with transgenic GFP reporter allele for β-catenin/Tcf transcription activity. Note that heterogeneous expressions of both β-catenin and GFP are observed in a colon tumour. (**B**) Double immunostaining for β-catenin and Ki-67 in a colon tumour. Tumor cells with strong β-catenin expression show less frequent staining for Ki-67. (**C**) Double immunostaining for Hes1 (green) and Ki-67 (red). Distinct localisation of Hes1-expressing cells and Ki-67-positive cells are seen in colon tumour. Arrows indicate cells with positive nuclear staining for Hes1. (**D**) Immunostaining for β-catenin and Hes1 in serial sections. Colocalisation of higher levels of β-catenin and Hes1 expression is observed in the colon tumour.

immunofluorescence staining revealed that β-catenin levels were well correlated with GFP intensity, demonstrating that different levels of β-catenin accumulation directly affect β-catenin/Tcf transcription in colonic tumours (Fig. 6A). Importantly, most tumour cells with nuclear β-catenin did not express Ki-67 (Fig. 6B), recapitulating our observations in β-catenin-overexpressing mice. When the intensity and localisation of β-catenin expression were examined by immunofluorescence staining, the majority of Ki-67-positive tumour cells showed cytoplasmic β-catenin expression (93.6%) rather than strong nuclear expression (6.4%). In addition to the heterogeneous pattern of nuclear β-catenin accumulation, expression of Hes1 was detectable only in a small subset of colon tumour cells (Fig. 6C,D). Co-staining for Ki-67 revealed that tumour cells with high levels of Hes1 do not divide actively (Fig. 6C). Furthermore, we found that cells with a nuclear β-catenin signal often exhibited high Hes1 expression (Fig. 6D), as we have seen in β-catenin-induced crypts (supplementary material Fig. S4). These findings indicate that colon tumours, like our β-catenin inducible mouse model, consist of heterogeneous populations of cells displaying different activities of canonical Wnt signalling, Notch signalling and cell proliferation.

DISCUSSION

Previous studies using conditional *Apc* knockout mice demonstrated that acute loss of the *Apc* gene rapidly expands progenitor cells in the intestinal crypts (Sansom et al., 2004; Andreu et al., 2005) but does not lead to crypt fission/branching, suggesting that Wnt activation through loss of *Apc* is not sufficient to induce *de novo* crypt formation. In the present study, we showed that high levels of β-catenin activation are sufficient for *de novo* crypt formation of adult mice (Fig. 2). Our observation suggests that β-catenin activation amplifies ISCs, which is consistent with recent work carried out in *Drosophila* hindgut (Takashima et al., 2008). The discrepancy between previous reports and our study seems to arise from differences in the levels of Wnt activation. In fact, by titrating down the levels of activated β-catenin, we also failed to induce *de novo* crypt formation but instead expanded the proliferating progenitor compartment of the crypts (Fig. 5A). These combined findings strongly suggest that high levels of the canonical Wnt effector β-catenin are required for ISC expansion, whereas low levels of activation can induce the active proliferation of progenitor cells. This notion is consistent with a recent finding, which demonstrated that different levels of Wnt signalling exert distinct roles on the self-renewal and differentiation potentials of haematopoietic stem cells (Luis et al., 2011).

The notion that *de novo* crypt formation and cell proliferation are controlled by distinct levels of β-catenin activation is reminiscent of previous observations from our laboratory on the two-stage tumorigenesis of the $Apc^{Min/+}$ mouse (Yamada et al., 2002; Oyama et al., 2008). In the colon of $Apc^{Min/+}$ mice, we detected many microadenomas as early as 3 weeks of age, of which only a limited number progressed to large tumours. Although early

microadenomas already harboured frequent loss of *Apc* and increased β-catenin/Tcf transcription, larger tumours exhibited further elevations of β-catenin/Tcf transcriptional activity, thus suggesting that increased β-catenin/Tcf signalling is required for the development of larger tumours. The dose-dependent effect of Wnt activation on intestinal tumorigenesis has also been implicated in mouse models with different hypomorphic *Apc* mutant alleles, supporting the requirement for higher levels of Wnt activation for intestinal tumorigenesis (Gaspar and Fodde, 2004). A series of previous studies demonstrated that epigenetic modifications associated with DNA methylation are involved in the transition from microadenomas to large tumours in the $Apc^{Min/+}$ mouse (Yamada et al., 2005; Lin et al., 2006; Linhart et al., 2007). In human colorectal cancers, it has been shown that epigenetic silencing of SFRPs, negative modifiers of Wnt signalling, are frequently found, and such inactivation can further activate the canonical Wnt signals in colon cancer cell lines with *APC* or *CTNNB1* mutations (Suzuki et al., 2004). It is therefore possible that activation of the canonical Wnt signalling by both genetic and epigenetic alterations enables colonic stem cells to expand, leading to *de novo* crypt formation, which ultimately results in tumour growth.

A number of signalling cascades have been implicated in the maintenance of intestinal homeostasis (Scoville et al., 2008), but it remains unclear how the Wnt signalling pathway connects with other signalling cascades within the intestine to control homeostasis. Here, we showed that canonical Wnt signalling plays an important role in *de novo* crypt formation in the colon, and that a higher level of β-catenin activation is crucial for Notch activation. Our finding that Notch inhibition prevented crypt fission/branching in β-catenin-induced colon indicates the requirement for Notch activation in β-catenin-induced *de novo* crypt formation (Fig. 4G; supplementary material Fig. S8A). Interestingly, β-catenin activation rapidly induced transcriptional activation of the Notch ligands *Jag1* and *Jag2*, and the Notch receptors *Notch1* and *Notch2* (Fig. 4B, Fig. 5B), thus offering a possible direct link between these two pathways. Together with previous findings that β-catenin induces *Jag1* transcription, leading to Notch activation in human colon cancer cell lines (Rodilla et al., 2009), it is therefore likely that the increased expression of Notch ligands by β-catenin induction causes Notch activation in the colonic epithelium. Furthermore, a recent study clearly demonstrated that Notch1 and Notch2 receptors are expressed specifically in ISCs (Fre et al., 2011; Sato et al., 2011). The increased expressions of Notch receptors could play a role in the induction of ISC-like cells by β-catenin induction (Fig. 4B). It is also noteworthy that the constitutive activation of Notch results in no obvious effect on β-catenin nuclear localisation (Fre et al., 2005). These findings indicate a hierarchical relationship between the Wnt and Notch signalling pathways in the intestinal epithelium. This hierarchy might explain why genetic alterations in colon cancers are frequently detected in the Wnt signalling pathway, but not in the Notch signalling pathway.

The failure of most current therapies to cure cancer has led to the hypothesis that treatments targeted at malignant proliferation spare a slowly cycling cancer stem cell population. In this study, higher levels of Wnt activation induced *de novo* crypt formation and induced crypt cells to acquire slow-cycling properties. Interestingly, our observation of a β-catenin-induced slow-cycling property is consistent with previous reports in human colorectal cancers. Human colourectal cancers showed heterogeneous intracellular distribution of β-catenin, and tumour cells with nuclear accumulation revealed low cell proliferation rates (Brabletz et al., 2001; Fodde and Brabletz, 2007). Importantly, we also found that colon tumours in $Apc^{Min/+}$ mice consist of heterogeneous cells displaying different levels of β-catenin accumulation and downstream gene expression (Fig. 6A), and tumour cells with nuclear β-catenin are dividing more slowly than surrounding tumour cells, suggesting that such cells are similar to cells at the crypt bottom of the normal colon. Thus, we propose that a hierarchical control of cell proliferation in the colonic crypt epithelium is retained to some extent in colonic neoplasms. Accordingly, we found that tumour cells with nuclear β-catenin are accompanied by high Notch signalling (Fig. 6D), as has been reported in crypt bottom cells (Kayahara et al., 2003). It is interesting to note that a γ-secretase inhibitor turned slow-cycling cells into actively proliferating cells (Fig. 4C-G; supplementary material Fig. S7A). A previous study showed that Notch inhibitors turn undifferentiated, proliferating cells into quiescent cells in colorectal neoplasias (van Es et al., 2005), indicating that the Notch inhibitor might be of therapeutic benefit in colorectal cancers. The discrepancy in the effects of Notch inhibitor could be explained by differences in states of the affected cells between proliferating progenitor cells and ISC-like cells. Although the previous study showed effects on the transition of proliferating cells into terminally differentiated quiescent cells, our data suggest that a Notch inhibitor may promote the transition of slow-cycling ISC-like cells into progenitor cells in the colon. Considering the chemoresistance of slow-cycling cancer stem cells, the results also suggest that Notch inhibitors combined with chemotherapeutic agents and/or irradiation might be effective as treatments targeting slow-cycling cancer stem cells in the colon.

In summary, our results indicate that, although proliferating progenitor cells in colonic crypts physiologically express higher levels of β-catenin/Tcf transcriptions, a further activation of the canonical Wnt singalling leads to *de novo* crypt formation, consisting of relatively slow-cycling cells in the adult colon, which is accompanied by activation of Notch signalling with transactivation of Notch ligands and receptors. However, treatment with a Notch/γ-secretase inhibitor turns such slow-cycling cells into proliferating cells, although we cannot exclude the possibility that some of the observed phenotypes are the result of superphysiological β-catenin expression obtained with our transgenic system. These findings suggest that Wnt and Notch signalling act in a synergistic and hierarchical manner to control differentiation and proliferation of the colonic crypt epithelium *in vivo*.

Acknowledgements
We thank Ayako Suga, Kyoko Takahashi, Huilan Zhi and Yoshitaka Kinjyo for technical assistance, and Hans Clevers for providing the S33 β-catenin overexpression vector.

Funding
This study is supported by PRESTO, Grants-in-Aid from the Ministry of Health, Labour and Welfare of Japan, and Ministry of Education, Culture, Sports, Science and Technology of Japan [Y.Y.]. J.U. is supported by grants of the German Cancer Aid and German Research Council [SFB873]. K.H. was supported by the National Institutes of Health [DP2OD003266 and R01HD058013]. Deposited in PMC for release after 12 months.

Competing interests statement
The authors declare no competing financial interests.

Supplementary material
Supplementary material available online at
http://dev.biologists.org/lookup/suppl/doi:10.1242/dev.084103/-/DC1

References

Andreu, P., Colnot, S., Godard, C., Gad, S., Chafey, P., Niwa-Kawakita, M., Laurent-Puig, P., Kahn, A., Robine, S., Perret, C. et al. (2005). Crypt-restricted proliferation and commitment to the Paneth cell lineage following Apc loss in the mouse intestine. *Development* **132**, 1443-1451.

Barker, N., van Es, J. H., Kuipers, J., Kujala, P., van den Born, M., Cozijnsen, M., Haegebarth, A., Korving, J., Begthel, H., Peters, P. J. et al. (2007). Identification of stem cells in small intestine and colon by marker gene Lgr5. *Nature* **449**, 1003-1007.

Beard, C., Hochedlinger, K., Plath, K., Wutz, A. and Jaenisch, R. (2006). Efficient method to generate single-copy transgenic mice by site-specific integration in embryonic stem cells. *Genesis* **44**, 23-28.

Brabletz, T., Jung, A., Reu, S., Porzner, M., Hlubek, F., Kunz-Schughart, L. A., Knuechel, R. and Kirchner, T. (2001). Variable beta-catenin expression in colorectal cancers indicates tumor progression driven by the tumor environment. *Proc. Natl. Acad. Sci. USA* **98**, 10356-10361.

Fevr, T., Robine, S., Louvard, D. and Huelsken, J. (2007). Wnt/beta-catenin is essential for intestinal homeostasis and maintenance of intestinal stem cells. *Mol. Cell. Biol.* **27**, 7551-7559.

Fodde, R. and Brabletz, T. (2007). Wnt/beta-catenin signaling in cancer stemness and malignant behavior. *Curr. Opin. Cell Biol.* **19**, 150-158.

Foudi, A., Hochedlinger, K., Van Buren, D., Schindler, J. W., Jaenisch, R., Carey, V. and Hock, H. (2009). Analysis of histone 2B-GFP retention reveals slowly cycling hematopoietic stem cells. *Nat. Biotechnol.* **27**, 84-90.

Fre, S., Huyghe, M., Mourikis, P., Robine, S., Louvard, D. and Artavanis-Tsakonas, S. (2005). Notch signals control the fate of immature progenitor cells in the intestine. *Nature* **435**, 964-968.

Fre, S., Hannezo, E., Sale, S., Huyghe, M., Lafkas, D., Kissel, H., Louvi, A., Greve, J., Louvard, D. and Artavanis-Tsakonas, S. (2011). Notch lineages and activity in intestinal stem cells determined by a new set of knock-in mice. *PLoS ONE* **6**, e25785.

Gaspar, C. and Fodde, R. (2004). APC dosage effects in tumorigenesis and stem cell differentiation. *Int. J. Dev. Biol.* **48**, 377-386.

Harada, N., Tamai, Y., Ishikawa, T., Sauer, B., Takaku, K., Oshima, M. and Taketo, M. M. (1999). Intestinal polyposis in mice with a dominant stable mutation of the beta-catenin gene. *EMBO J.* **18**, 5931-5942.

He, X. C., Yin, T., Grindley, J. C., Tian, Q., Sato, T., Tao, W. A., Dirisina, R., Porter-Westpfahl, K. S., Hembree, M., Johnson, T. et al. (2007). PTEN-deficient intestinal stem cells initiate intestinal polyposis. *Nat. Genet.* **39**, 189-198.

Ito, T., Udaka, N., Yazawa, T., Okudela, K., Hayashi, H., Sudo, T., Guillemot, F., Kageyama, R. and Kitamura, H. (2000). Basic helix-loop-helix transcription factors regulate the neuroendocrine differentiation of fetal mouse pulmonary epithelium. *Development* **127**, 3913-3921.

Jung, A., Schrauder, M., Oswald, U., Knoll, C., Sellberg, P., Palmqvist, R., Niedobitek, G., Brabletz, T. and Kirchner, T. (2001). The invasion front of human colorectal adenocarcinomas shows co-localization of nuclear beta-catenin, cyclin D1, and p16INK4A and is a region of low proliferation. *Am. J. Pathol.* **159**, 1613-1617.

Kaneko, Y., Sakakibara, S., Imai, T., Suzuki, A., Nakamura, Y., Sawamoto, K., Ogawa, Y., Toyama, Y., Miyata, T. and Okano, H. (2000). Musashi1: an evolutionally conserved marker for CNS progenitor cells including neural stem cells. *Dev. Neurosci.* **22**, 139-153.

Kayahara, T., Sawada, M., Takaishi, S., Fukui, H., Seno, H., Fukuzawa, H., Suzuki, K., Hiai, H., Kageyama, R., Okano, H. et al. (2003). Candidate markers for stem and early progenitor cells, Musashi-1 and Hes1, are expressed in crypt base columnar cells of mouse small intestine. *FEBS Lett.* **535**, 131-135.

Korinek, V., Barker, N., Moerer, P., van Donselaar, E., Huls, G., Peters, P. J. and Clevers, H. (1998). Depletion of epithelial stem-cell compartments in the small intestine of mice lacking Tcf-4. *Nat. Genet.* **19**, 379-383.

Kuhnert, F., Davis, C. R., Wang, H. T., Chu, P., Lee, M., Yuan, J., Nusse, R. and Kuo, C. J. (2004). Essential requirement for Wnt signaling in proliferation of adult small intestine and colon revealed by adenoviral expression of Dickkopf-1. *Proc. Natl. Acad. Sci. USA* **101**, 266-271.

Li, L. and Clevers, H. (2010). Coexistence of quiescent and active adult stem cells in mammals. *Science* **327**, 542-545.

Lin, H., Yamada, Y., Nguyen, S., Linhart, H., Jackson-Grusby, L., Meissner, A., Meletis, K., Lo, G. and Jaenisch, R. (2006). Suppression of intestinal neoplasia by deletion of Dnmt3b. *Mol. Cell. Biol.* **26**, 2976-2983.

Linhart, H. G., Lin, H., Yamada, Y., Moran, E., Steine, E. J., Gokhale, S., Lo, G., Cantu, E., Ehrich, M., He, T. et al. (2007). Dnmt3b promotes tumorigenesis *in vivo* by gene-specific *de novo* methylation and transcriptional silencing. *Genes Dev.* **21**, 3110-3122.

Luis, T. C., Naber, B. A., Roozen, P. P., Brugman, M. H., de Haas, E. F., Ghazvini, M., Fibbe, W. E., van Dongen, J. J., Fodde, R. and Staal, F. J. (2011). Canonical wnt signaling regulates hematopoiesis in a dosage-dependent fashion. *Cell Stem Cell* **9**, 345-356.

Morin, P. J., Sparks, A. B., Korinek, V., Barker, N., Clevers, H., Vogelstein, B. and Kinzler, K. W. (1997). Activation of beta-catenin-Tcf signaling in colon cancer by mutations in beta-catenin or APC. *Science* **275**, 1787-1790.

Oyama, T., Yamada, Y., Hata, K., Tomita, H., Hirata, A., Sheng, H., Hara, A., Aoki, H., Kunisada, T., Yamashita, S. et al. (2008). Further upregulation of beta-catenin/Tcf transcription is involved in the development of macroscopic tumors in the colon of ApcMin/+ mice. *Carcinogenesis* **29**, 666-672.

Pinto, D., Gregorieff, A., Begthel, H. and Clevers, H. (2003). Canonical Wnt signals are essential for homeostasis of the intestinal epithelium. *Genes Dev.* **17**, 1709-1713.

Potten, C. S., Booth, C., Tudor, G. L., Booth, D., Brady, G., Hurley, P., Ashton, G., Clarke, R., Sakakibara, S. and Okano, H. (2003). Identification of a putative intestinal stem cell and early lineage marker; musashi-1. *Differentiation* **71**, 28-41.

Rodilla, V., Villanueva, A., Obrador-Hevia, A., Robert-Moreno, A., Fernández-Majada, V., Grilli, A., López-Bigas, N., Bellora, N., Albà, M. M., Torres, F. et al. (2009). Jagged1 is the pathological link between Wnt and Notch pathways in colorectal cancer. *Proc. Natl. Acad. Sci. USA* **106**, 6315-6320.

Sangiorgi, E. and Capecchi, M. R. (2008). Bmi1 is expressed *in vivo* in intestinal stem cells. *Nat. Genet.* **40**, 915-920.

Sansom, O. J., Reed, K. R., Hayes, A. J., Ireland, H., Brinkmann, H., Newton, I. P., Batlle, E., Simon-Assmann, P., Clevers, H., Nathke, I. S. et al. (2004). Loss of Apc *in vivo* immediately perturbs Wnt signaling, differentiation, and migration. *Genes Dev.* **18**, 1385-1390.

Sato, T., van Es, J. H., Snippert, H. J., Stange, D. E., Vries, R. G., van den Born, M., Barker, N., Shroyer, N. F., van de Wetering, M. and Clevers, H. (2011). Paneth cells constitute the niche for Lgr5 stem cells in intestinal crypts. *Nature* **469**, 415-418.

Scoville, D. H., Sato, T., He, X. C. and Li, L. (2008). Current view: intestinal stem cells and signaling. *Gastroenterology* **134**, 849-864.

Suzuki, H., Watkins, D. N., Jair, K. W., Schuebel, K. E., Markowitz, S. D., Chen, W. D., Pretlow, T. P., Yang, B., Akiyama, Y., Van Engeland, M. et al. (2004). Epigenetic inactivation of SFRP genes allows constitutive WNT signaling in colorectal cancer. *Nat. Genet.* **36**, 417-422.

Takashima, S., Mkrtchyan, M., Younossi-Hartenstein, A., Merriam, J. R. and Hartenstein, V. (2008). The behaviour of Drosophila adult hindgut stem cells is controlled by Wnt and Hh signalling. *Nature* **454**, 651-655.

Takeda, N., Jain, R., LeBoeuf, M. R., Wang, Q., Lu, M. M. and Epstein, J. A. (2011). Interconversion between intestinal stem cell populations in distinct niches. *Science* **334**, 1420-1424.

Tsukamoto, T., Fukami, H., Yamanaka, S., Yamaguchi, A., Nakanishi, H., Sakai, H., Aoki, I. and Tatematsu, M. (2001). Hexosaminidase-altered aberrant crypts, carrying decreased hexosaminidase alpha and beta subunit mRNAs, in colon of 1,2-dimethylhydrazine-treated rats. *Jpn. J. Cancer Res.* **92**, 109-118.

Tumbar, T., Guasch, G., Greco, V., Blanpain, C., Lowry, W. E., Rendl, M. and Fuchs, E. (2004). Defining the epithelial stem cell niche in skin. *Science* **303**, 359-363.

van de Wetering, M., Sancho, E., Verweij, C., de Lau, W., Oving, I., Hurlstone, A., van der Horn, K., Batlle, E., Coudreuse, D., Haramis, A. P. et al. (2002). The beta-catenin/TCF-4 complex imposes a crypt progenitor phenotype on colorectal cancer cells. *Cell* **111**, 241-250.

van der Flier, L. G., Sabates-Bellver, J., Oving, I., Haegebarth, A., De Palo, M., Anti, M., Van Gijn, M. E., Suijkerbuijk, S., Van de Wetering, M., Marra, G. et al. (2007). The Intestinal Wnt/TCF Signature. *Gastroenterology* **132**, 628-632.

van der Flier, L. G., van Gijn, M. E., Hatzis, P., Kujala, P., Haegebarth, A., Stange, D. E., Begthel, H., van den Born, M., Guryev, V., Oving, I. et al. (2009). Transcription factor achaete scute-like 2 controls intestinal stem cell fate. *Cell* **136**, 903-912.

van Es, J. H., van Gijn, M. E., Riccio, O., van den Born, M., Vooijs, M., Begthel, H., Cozijnsen, M., Robine, S., Winton, D. J., Radtke, F. et al. (2005). Notch/gamma-secretase inhibition turns proliferative cells in intestinal crypts and adenomas into goblet cells. *Nature* **435**, 959-963.

van Noort, M., van de Wetering, M. and Clevers, H. (2002). Identification of two novel regulated serines in the N terminus of beta-catenin. *Exp. Cell Res.* 276, 264-272.

Vermeulen, L., De Sousa E Melo, F., van der Heijden, M., Cameron, K., de Jong, J. H., Borovski, T., Tuynman, J. B., Todaro, M., Merz, C., Rodermond, H. et al. (2010). Wnt activity defines colon cancer stem cells and is regulated by the microenvironment. *Nat. Cell Biol.* **12**, 468-476.

Yamada, Y., Hata, K., Hirose, Y., Hara, A., Sugie, S., Kuno, T., Yoshimi, N., Tanaka, T. and Mori, H. (2002). Microadenomatous lesions involving loss of Apc heterozygosity in the colon of adult Apc(Min/+) mice. *Cancer Res.* **62**, 6367-6370.

Yamada, Y., Jackson-Grusby, L., Linhart, H., Meissner, A., Eden, A., Lin, H. and Jaenisch, R. (2005). Opposing effects of DNA hypomethylation on intestinal and liver carcinogenesis. *Proc. Natl. Acad. Sci. USA* **102**, 13580-13585.

Yamashita, S., Nomoto, T., Ohta, T., Ohki, M., Sugimura, T. and Ushijima, T. (2003). Differential expression of genes related to levels of mucosal cell proliferation among multiple rat strains by using oligonucleotide microarrays. *Mamm. Genome* **14**, 845-852.

Research article

EWS/ATF1 expression induces sarcomas from neural crest–derived cells in mice

Kazunari Yamada,[1,2] Takatoshi Ohno,[1] Hitomi Aoki,[3] Katsunori Semi,[4,5] Akira Watanabe,[4,5] Hiroshi Moritake,[6] Shunichi Shiozawa,[7] Takahiro Kunisada,[3] Yukiko Kobayashi,[8] Junya Toguchida,[4,8,9] Katsuji Shimizu,[1] Akira Hara,[2] and Yasuhiro Yamada[2,4,5]

[1]Department of Orthopedic Surgery, [2]Department of Tumor Pathology, and [3]Department of Tissue and Organ Development Regeneration and Advanced Medical Science, Gifu University Graduate School of Medicine, Gifu, Japan.
[4]Center for iPS Cell Research and Application (CiRA) and [5]Institute for Integrated Cell-Material Sciences, (WPI-iCeMS), Kyoto University, Kyoto, Japan.
[6]Division of Pediatrics, Department of Reproductive and Developmental Medicine, Faculty of Medicine, University of Miyazaki, Miyazaki, Japan.
[7]Department of Medicine, Kyushu University Beppu Hospital, Beppu, Japan. [8]Department of Tissue Regeneration, Institute for Frontier Medical Sciences, and [9]Department of Orthopaedic Surgery, Kyoto University, Kyoto, Japan.

Clear cell sarcoma (CCS) is an aggressive soft tissue malignant tumor characterized by a unique t(12;22) translocation that leads to the expression of a chimeric *EWS/ATF1* fusion gene. However, little is known about the mechanisms underlying the involvement of *EWS/ATF1* in CCS development. In addition, the cellular origins of CCS have not been determined. Here, we generated *EWS/ATF1*-inducible mice and examined the effects of *EWS/ATF1* expression in adult somatic cells. We found that forced expression of *EWS/ATF1* resulted in the development of *EWS/ATF1*-dependent sarcomas in mice. The histology of *EWS/ATF1*-induced sarcomas resembled that of CCS, and *EWS/ATF1*-induced tumor cells expressed CCS markers, including S100, SOX10, and MITF. Lineage-tracing experiments indicated that neural crest–derived cells were subject to *EWS/ATF1*-driven transformation. EWS/ATF1 directly induced Fos in an ERK-independent manner. Treatment of human and *EWS/ATF1*-induced CCS tumor cells with FOS-targeted siRNA attenuated proliferation. These findings demonstrated that FOS mediates the growth of *EWS/ATF1*-associated sarcomas and suggest that FOS is a potential therapeutic target in human CCS.

Introduction

Clear cell sarcoma (CCS) is an aggressive malignancy of adolescents and young adults that was first described by Enzinger (1). It typically arises in the deep soft tissues of the lower extremities closed to tendon, fascia, and aponeurosis (2). Chemotherapy and radiotherapy are not of any benefit (3–5), and a high rate of local and distant recurrence results in poor survival rates (3, 6, 7). CCSs harbor the potential for melanocytic differentiation and melanin synthesis (8). Gene expression profiles support the classification of CCS as a distinct genomic subtype of melanomas (9). These melanocytic features often make the distinction from malignant melanoma (MM) difficult. However, in contrast to MM, CCS is characterized by a chromosomal translocation, t(12;22)(q13;q12), that leads to the fusion of activating transcription factor 1 (*ATF1*) gene localized to 12q13 to Ewing's sarcoma oncogene (*EWS*) gene at 22q12 in up to 90% of cases, resulting in expression of the *EWS/ATF1* fusion gene (10–12). Given that CCS and MM have such similar characteristics, it has been proposed that CCSs may arise from a neural crest progenitor. However, the exact origin of CCS still remains to be determined.

The biological role of the EWS/ATF1 fusion protein is still unclear. EWS contains a transcriptional activation domain in the N-terminal region (13–15) and several conserved RNA binding motifs in the C-terminal region (16). Binding of the N-terminal region of EWS to the RNA polymerase II subunit hsRPB7 has been proposed to be important for transactivation of the target genes (17). In contrast, ATF1 is a member of the CREB transcription factor family, whose activity is regulated through phosphorylation of its kinase inducible domain (KID) by protein kinase A (18). ATF1 mediates the activation of cAMP-responsive genes through binding to a conserved cAMP-responsive element (CRE) as a dimmer (19, 20). However, the N-terminal activation domain of EWS replaces the KID in the EWS/ATF1 fusion protein, rendering it unable to support a typical inductive signal (21). Therefore, EWS/ATF1 can act as constitutive transcriptional activator in a cAMP-independent fashion with normal CRE DNA binding activity (14, 22, 23).

Previous studies have revealed some target genes of EWS/ATF1, but their true function in tumorigenesis is still not well understood (24). Expression of *MITF* is constitutively activated by *EWS/ATF1* in CCS in vitro (25). Consistent with this finding, several studies have identified the expression of MITF protein or mRNA in CCS (26–28). MITF is a master regulator of melanocyte development and plays a role in melanoma development (29, 30). Importantly, activation of MITF by EWS/ATF1 is required for CCS proliferation as well as for melanocytic differentiation of CCS in vitro (25).

Although previous studies have demonstrated that EWS/ATF1 is associated with oncogenic potential in CCS, the effect of in vivo expression of *EWS/ATF1* on sarcoma formation is still not known. In the present study, we established *EWS/ATF1* transgenic mice using a doxycycline-dependent expression system in order to investigate the role of *EWS/ATF1* on CCS development in vivo. Our results showed that forced expression of *EWS/ATF1* induced CCS-like sarcoma in the transgenic mice. This mouse model was used to identify the origin of *EWS/ATF1*-induced sarcomas as well as the direct target of EWS/ATF1 in these sarcomas.

Results

Inducible expression of EWS/ATF1 in mice. We first generated doxycycline-inducible *EWS/ATF1* ES cells, in which the human *EWS/ATF1* type 2 fusion gene (26, 31) can be induced under the control of

Conflict of interest: The authors have declared that no conflict of interest exists.
Citation for this article: *J Clin Invest.* 2013;123(2):600–610. doi:10.1172/JCI63572.

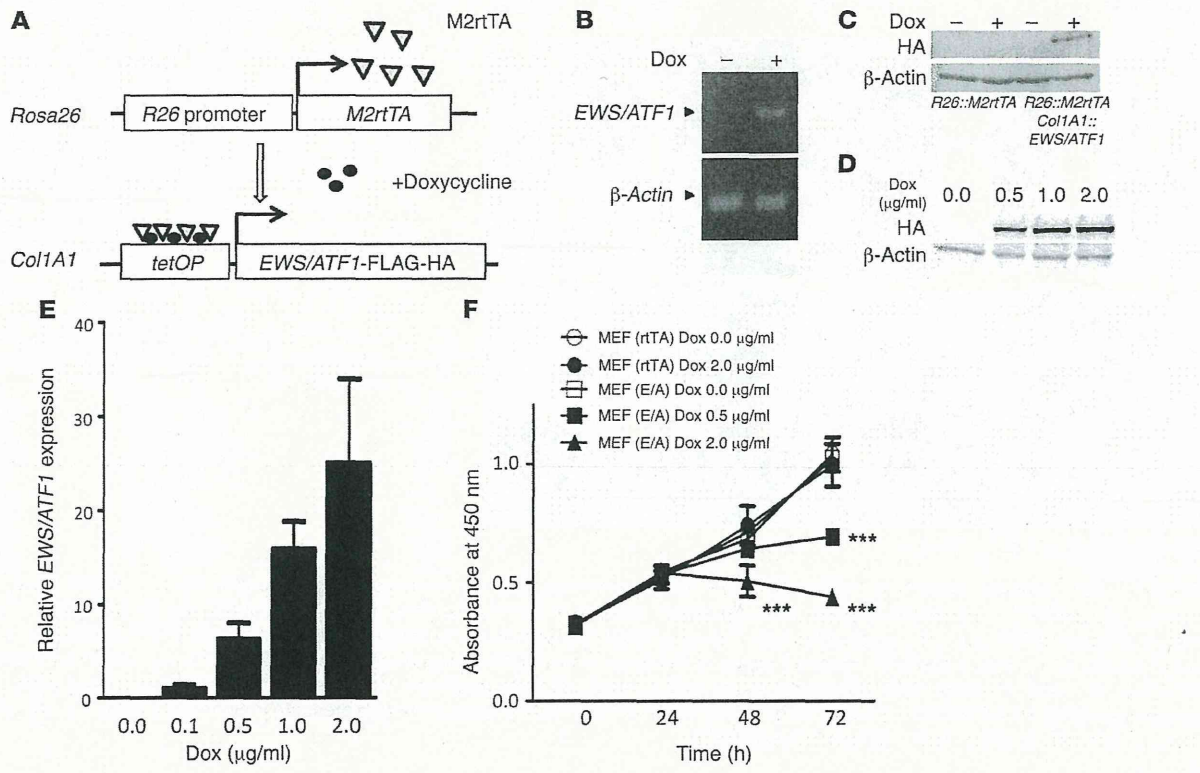

Figure 1

Inducible expression of *EWS/ATF1*. (**A**) Schematic of the doxycycline-inducible *EWS/ATF1* alleles. (**B**) *EWS/ATF1* expression in ES cells, detected by RT-PCR, after exposure to doxycycline for 12 hours. (**C**) EWS/ATF1 expression in ES cells, detected by Western blot, after exposure to doxycycline for 24 hours. (**D**) Dose-dependent induction of EWS/ATF1 protein in *EWS/ATF1*-inducible ES cells by doxycycline. ES cells were exposed to doxycycline concentrations up to 2 μg/ml for 24 hours. Western blot analysis was performed using an anti-HA antibody. (**E**) Dose-dependent doxycycline induction of *EWS/ATF1* mRNA in *EWS/ATF1*-inducible MEFs. MEFs were exposed to different concentrations of doxycycline for 24 hours. Transcript levels were normalized to β-*actin*. Data are mean ± SD ($n = 3$). (**F**) *EWS/ATF1* expression suppressed MEF growth. Cell viability was determined by WST-8 assay. Data are mean ± SD ($n = 4$). Control MEFs (rtTA) and *EWS/ATF1*-inducible MEFs (E/A) were derived from heterozygous *Rosa26::M2rtTA* and *Col1A1::tetO-EWS/ATF1* mice, respectively. ***$P < 0.001$ vs. MEF (rtTA) Dox 0.0 μg/ml, MEF (rtTA) Dox 2.0 μg/ml, and MEF (E/A) Dox 0.0 μg/ml.

a tetracycline-responsive regulatory element (Figure 1A). Upon treatment of these ES cells with doxycycline, expression of the *EWS/ATF1* fusion transcript was detected by RT-PCR (Figure 1B). We also confirmed the expression of EWS/ATF1 protein upon doxycycline treatment (Figure 1C), which was regulated in a dose-dependent manner (up to 2 μg/ml; Figure 1D).

Heterozygous *Rosa26::M2rtTA* mice with heterozygous *tetO-EWS/ATF1* allele were used to induce the *EWS/ATF1* fusion gene. Cultured murine embryonic fibroblasts (MEFs) derived from *EWS/ATF1*-inducible mice were first exposed to doxycycline to test the effect of *EWS/ATF1* expression on somatic cells. *EWS/ATF1* expression at the mRNA level was confirmed 24 hours after exposure (Figure 1E). Unexpectedly, the cell proliferation rate of MEFs decreased after *EWS/ATF1* induction in a doxycycline dose–dependent manner (Figure 1F).

EWS/ATF1 induces sarcoma formation in mice. To investigate the effect of *EWS/ATF1* expression in vivo, we treated *EWS/ATF1*-inducible mice at 6 weeks of age with doxycycline in the drinking water (50 μg/ml). The *EWS/ATF1*-inducible mice given doxycycline started to develop multiple macroscopic soft tissue tumors after 4 weeks. After doxycycline treatment, EWS/ATF1 protein was detected in a variety of tissues, including the intestine, liver, epidermis, and deep soft tissue (Supplemental Figure 1A; supplemental material available online with this article; doi:10.1172/JCI63572DS1). Doxycycline treatment for 3 months resulted in tumor formation in the deep soft tissues of all mice ($n = 39$), whereas control mice without doxycycline treatment developed no detectable tumors. *EWS/ATF1*-induced tumors typically arose in the trunks, heads, limbs, and whisker pads (Figure 2A). Macroscopically, tumors consisted of circumscribed and lobulated gray-white mass (Figure 2A). In most cases, the tumors were attached to fascia or aponeuroses (Figure 2, A and B), which indicates that the tumors specifically arose from the deep soft tissues. Importantly, 36 of 39 mice (92%) developed tumors in the trunk, which suggests that cells located in the trunk are particularly permissive for tumorigenesis by *EWS/ATF1* expression. Despite expression of EWS/ATF1 protein, no tumor formation was observed in other tissues, such as the epidermis and intestine, even in mice given doxycycline for 3 months.

Microscopic examination of these tumors revealed striking similarities to human CCSs. The tumors showed a rather uniform pattern of compact nests or fascicles of rounded or fusiform cells, which were divided by a framework of fibrocollagenous tissue (Figure 2B).

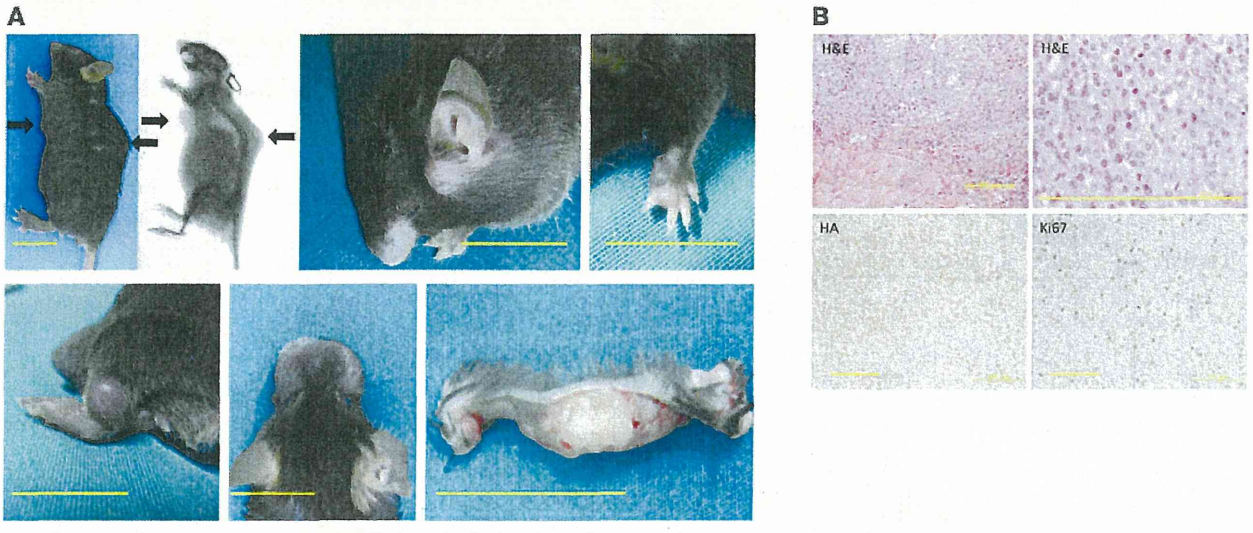

Figure 2
EWS/ATF1-induced tumors resemble human CCS. *EWS/ATF1* transgenic mice were administered 50 μg/ml doxycycline in their drinking water for 3 months. (**A**) *EWS/ATF1* expression caused tumor formation (arrows) in various locations: trunk, head, limbs, and whisker pads. X-ray examination revealed multiple tumors in deep soft tissue. The cut surface of a large tumor on the ventral trunk of an *EWS/ATF1*-inducible mouse revealed a lobulated gray-white mass in the deep soft tissue. Scale bars: 20 mm. (**B**) Histological analysis of *EWS/ATF1*-induced tumors. Tumors were composed of round or fusiform cells with prominent basophilic nuclei and clear cytoplasm, which were surrounded by fibrous fascicles. HA immunostaining confirmed EWS/ATF1 expression in the tumor cells. Frequent Ki67-positive cells were present throughout the lesions. Scale bars: 200 μm (H&E, left); 50 μm (H&E, right); 100 μm (HA and Ki67).

The individual tumor cells had a homogeneous appearance. They had round to ovoid vesicular nuclei with prominent basophilic nucleoli and clear or pale-staining cytoplasm (Figure 2B). The majority of the tumor cells expressed EWS/ATF1 fusion protein in nuclei (Figure 2B and Supplemental Figure 2A). Ki67-positive proliferating cells were observed in about 30%–40% of tumor cells (Figure 2B), indicative of active proliferative activity. The survival curves of *EWS/ATF1*-induced mice were analyzed to evaluate the overall effect of *EWS/ATF1* expression on life span. The transgenic mice treated with doxycycline became moribund within 3–10 months, suggestive of multiple tumor formation in the deep soft tissue, whereas mice without doxycycline treatment survived much longer, and no tumor formation was observed. The median survival time of *EWS/ATF1*-inducible mice treated with doxycycline was 20 weeks (Supplemental Figure 2B).

Previous studies demonstrated that human CCSs express markers for neural crest lineage as well as melanocytic differentiation (8, 9). Therefore, to examine the similarity of mouse *EWS/ATF1*-induced tumors with human CCSs, we performed immunohistochemical analysis for CCS-expressing markers; *EWS/ATF1*-induced tumor cells showed the expression such markers, including S100, Sox10, and Mitf (Figure 3A).

Neural crest–lineage cells are permissive to EWS/ATF1-driven sarcoma development. The cell of origin for CCS remains to be determined. Based on the potential of CCSs for melanocytic differentiation and melanin synthesis, previous studies proposed that CCS may arise from a neural crest progenitor. To determine whether *EWS/ATF1*-induced sarcomas actually arise from neural crest–derived cells, we performed a lineage-tracing experiment in which neural crest–derived cells were tagged by reporter in vivo (32). To label neural crest–derived cells in vivo, we first used transgenic mice containing *Wnt1-Cre* and floxed *LacZ* reporter alleles. We further introduced doxycycline-inducible *EWS/ATF1* alleles into the reporter mice to generate compound transgenic mice (Figure 3B). We confirmed that *EWS/ATF1*-induced tumor cells did not express *Wnt1* (Supplemental Figure 3A). Transgenic mice were treated with doxycycline in the drinking water to induce subcutaneous tumors and the developed tumors were then analyzed for the expression of the reporter gene. Importantly, all 14 *EWS/ATF1*-induced tumors were ubiquitously positive for X-gal staining (Figure 3C and Supplemental Figure 3D), which suggests that neural crest–lineage cells are a cell of origin for *EWS/ATF1*-associated sarcomas. We further performed another lineage-tracing experiment using transgenic mice containing *P0-Cre* and floxed *EYFP* reporter alleles (Figure 3D), which have been also widely used to label neural crest–derived cells. Again, we found that all 6 *EWS/ATF1*-induced tumors were positive for EYFP (Figure 3E and Supplemental Figure 4, C and D).

Establishment of tumor cell lines. Tumor samples were obtained from primary tumors of *EWS/ATF1*-induced mice to establish cell lines from *EWS/ATF1*-induced tumors. We established 2 tumor cell lines, G1297 and G1169, from 2 independent mice. These cells grew in the form of an adherent monolayer in the presence of doxycycline (0.2 μg/ml). We cultured the cells up to the fourth passage in medium containing 0.2 μg/ml doxycycline in order to avoid contamination by fibroblasts. We examined the effect of different concentrations of doxycycline on the growth and morphology of the established cell lines. We confirmed that the expression of *EWS/ATF1* transcript and protein increased in response to doxycycline in a dose-dependent manner in both established cell lines (Supplemental Figure 5, A–C). The growth and morphology of the tumor cells varied in a doxycycline dose–dependent manner: small, round tumor cells grew rapidly at concentrations above 0.1 μg/ml,

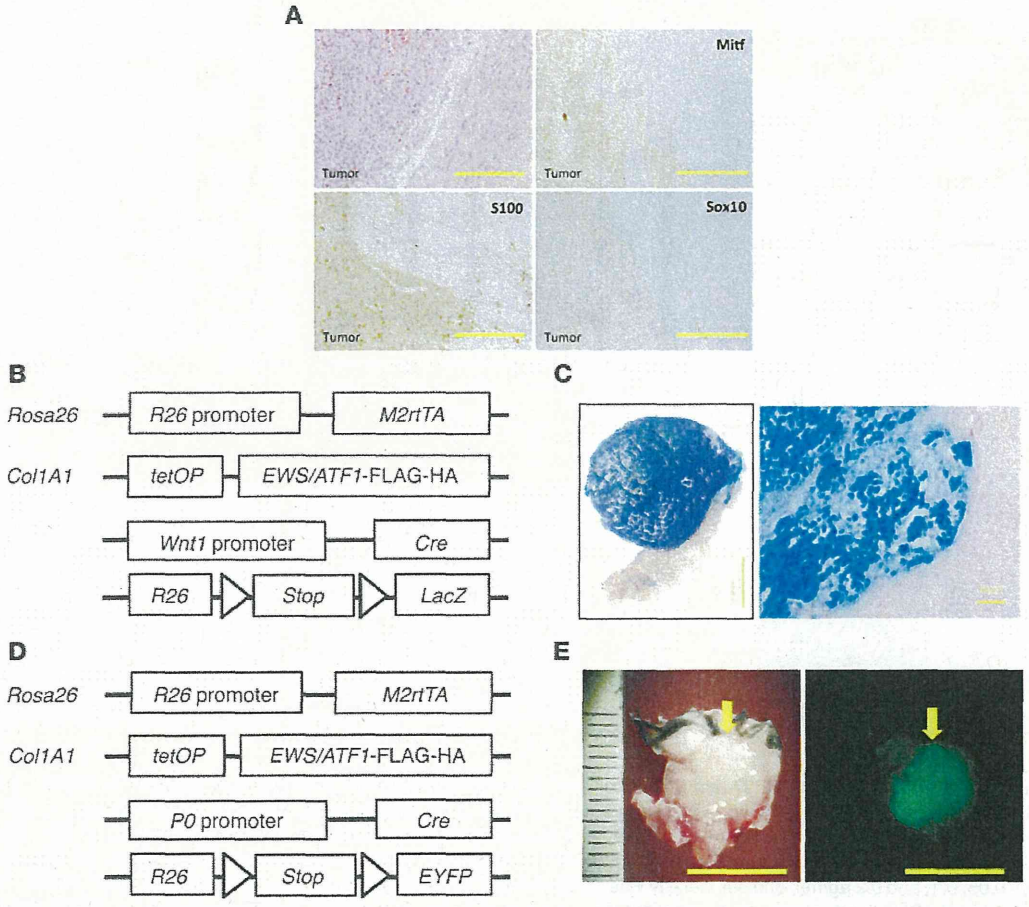

Figure 3

EWS/ATF1-induced tumors arise from neural crest–lineage cells. (**A**) Immunohistochemical analysis for CCS markers. Nuclear staining for S100, Sox10, and Mitf was observed in tumor cells. Sections were counterstained with hematoxylin. Scale bars: 100 μm. (**B**) Schematic representation of reporter alleles for the lineage-tracing experiment using *Wnt1-Cre* allele. Doxycycline-inducible *EWS/ATF1* alleles were introduced into reporter mice containing the *Wnt1-Cre* and floxed *LacZ* reporter alleles. (**C**) X-gal staining for *EWS/ATF1*-induced tumors with *Wnt1-Cre* and floxed *LacZ* reporter alleles. Positive staining for X-gal indicated that the tumor arose from a neural crest–lineage cell. Histological analysis revealed that neoplastic cells were stained with X-gal. Counterstaining was performed with fast red. Scale bars: 2 mm (left); 50 μm (right). (**D**) Schematic representation of reporter alleles for the lineage-tracing experiment using *P0-Cre* allele. Doxycycline-inducible *EWS/ATF1* alleles were introduced into reporter mice containing the *P0-Cre* and floxed *EYFP* reporter alleles. (**E**) Representative image of a tumor (arrow) in the trunk of an *EWS/ATF1*-induced mouse with *P0-Cre* and floxed *EYFP* reporter alleles. Fluorescent signals for EYFP expression were detected in the. Scale bars: 10 mm.

whereas dendritic fibroblast–like spindle cells were observed below 0.05 μg/ml (Figure 4A). Notably, doxycycline withdrawal caused rapid morphological changes, into a fibroblast-like shape, and these tumor cells did not proliferate up to the next passage (Figure 4A). Consistent with these findings, cell viability assay revealed that the number of cells was increased by doxycycline treatment in a dose-dependent manner (Figure 4B). We next examined the effect of *EWS/ATF1* expression on tumorigenesis ability in the subcutaneous tissue of immunocompromised mice. The established cell line G1297 was cultured in medium containing 0.2 μg/ml doxycycline, and 5.0×10^6 cells were transplanted into the subcutaneous tissue of nude mice. It is important to note that all mice treated with 50 μg/ml doxycycline in the drinking water developed tumors within 3 weeks, whereas no tumor formation was observed in mice without doxycycline treatment (Figure 4C). Histological analysis revealed that the subcutaneous tumors in nude mice consisted of neoplastic cells that resembled the primary tumor cells in *EWS/ATF1*-induced transgenic mice (Figure 4D). Positive immunoreactivity for HA-Tag was observed in all tumor cells (Figure 4D).

Continuous expression of EWS/ATF1 is required for tumor growth maintenance. To further examine whether continuous expression of *EWS/ATF1* is necessary for the growth of *EWS/ATF1*-induced tumors, we withdrew doxycycline in tumor-bearing EWS/ATF1 transgenic mice that had been given doxycycline for 3 months. Importantly, doxycycline withdrawal resulted in a rapid reduction of tumor mass in 4 independent mice (7 tumors total). The regressed tumors contained fibrous tissue, but no viable neoplastic cells were observed 3 months after doxycycline withdrawal (Figure 4E), which suggests that *EWS/ATF1*-induced tumor growth depends on continuous *EWS/ATF1* expression. We next examined the histological changes shortly after doxycycline withdrawal in order to investigate the mechanisms of tumor regression.

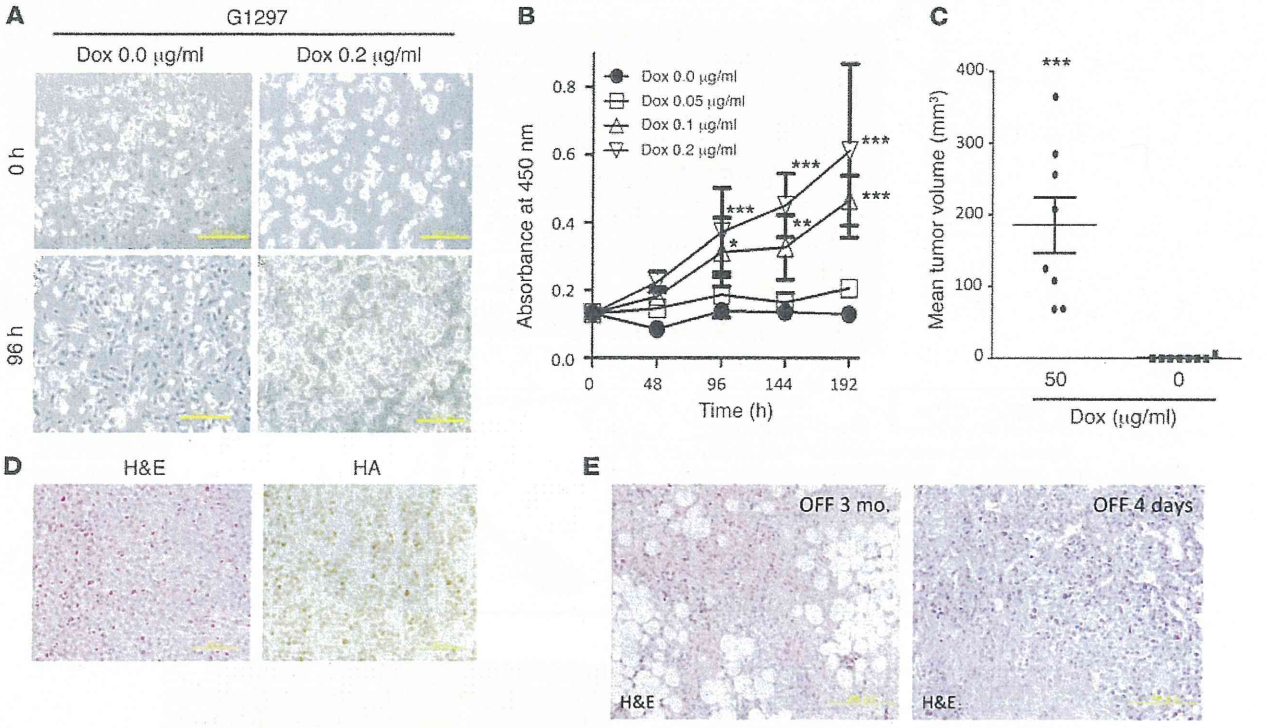

Figure 4

Establishment and analysis of tumor cell lines. G1297 and G1169 cell lines were established from 2 independent *EWS/ATF1*-induced tumors. (**A**) Morphology of the G1297 line after treatment without or with doxycycline (0 and 0.2 μg/ml, respectively). At concentrations above 0.1 μg/ml, small, round tumor cells grew rapidly, while dendritic fibroblast-like spindle cells were observed; tumor cell growth almost stopped at concentrations less than 0.05 μg/ml. Scale bars: 50 μm. (**B**) Effect of different levels of *EWS/ATF1* on tumor cell growth. G1297 cells were cultured in different concentrations of doxycycline (0, 0.05, 0.1, and 0.2 μg/ml), and cell viability was determined by WST-8 assay. Data are mean ± SD ($n = 8$). $^*P < 0.05$, $^{**}P < 0.01$, $^{***}P < 0.001$ vs. Dox 0.0 μg/ml. (**C**) Subcutaneous transplantation of 5.0×10^6 G1297 cells in immunocompromised mice resulted in tumor formation in mice treated with 50 μg/ml doxycycline ($n = 8$). Mean tumor volumes ± SEM are shown. $^{***}P < 0.005$. (**D**) Representative histology and HA immunostaining of tumors in nude mice. The tumor resembled the original sarcoma with EWS/ATF1 expression. Scale bars: 100 μm. (**E**) Doxycycline withdrawal led to rapid tumor regression. At 3 months after doxycycline withdrawal, no viable tumor cells were observed, and tumors were replaced by fibrous tissue. Widespread cell death was observed 4 days after doxycycline withdrawal. Scale bars: 200 μm.

We found widespread cell death within the tumor mass, accompanied by massive infiltration of inflammatory cells, at 4 days after doxycycline withdrawal (Figure 4E), which indicates that neoplastic cells cannot survive in vivo without *EWS/ATF1* expression. Taken together, these results clearly indicate that *EWS/ATF1* plays a pivotal role in the proliferation and maintenance of *EWS/ATF1*-induced tumor cells in vivo.

Fos is a direct target of EWS/ATF1. To determine the downstream targets regulated by EWS/ATF1, we next performed gene expression analysis using G1297 cells. First, we confirmed that withdrawal of doxycycline for 96 hours resulted in no detectable expression of *EWS/ATF1* RNA or protein in cultured tumor cells. Next, the tumor cells were exposed again to doxycycline at a concentration of 0.05 or 0.2 μg/ml, and microarray analysis was performed at 3 and 48 hours after doxycycline exposure. Induction of *EWS/ATF1* resulted in altered expression of a number of genes associated with cell growth, such as growth factor genes (*Areg* and *Ereg*), cell cycle regulators (*Cenpa*, *Ccna2*, *Ccnb2*, *Cdkn1b*, *Plk1*, and *Aurka*), and a proto-oncogene (*Fos*) at either time point (Supplemental Figure 6A). Although a previous study demonstrated that *MITF-M* is a direct target of EWS/ATF1 in human CCS cell lines (25), we failed to detect its expression in our *EWS/ATF1*-induced tumor cell lines and primary tumor samples (Supplemental Figure 7, A and B). Among the transcripts upregulated by *EWS/ATF1*, we focused on the proto-oncogene *Fos*, because this was one of the most highly upregulated genes by *EWS/ATF1* after doxycycline exposure in the microarray analysis (Supplemental Figure 6A). Quantitative real-time RT-PCR (qRT-PCR) confirmed upregulation of both *Fos* and *EWS/ATF1* transgenes in 2 independent tumor cell lines as early as 3 hours after doxycycline exposure (Figure 5A and Supplemental Figure 7C). We also found that the *EWS/ATF1*-induced tumor specimens expressed higher levels of both *Fos* and *EWS/ATF1* transgenes (Figure 5B). Expression of *Fos* is induced by numerous stimuli, which are transmitted through the RAS/Raf/MAP kinase or cAMP-dependent protein kinase pathway (33). In order to investigate the mechanism of *Fos* induction by *EWS/ATF1*, we next examined whether the RAS/Raf/MAP kinase pathway is involved in *EWS/ATF1*-mediated *Fos* activation. In contrast to the rapid and transient induction of Fos in MEFs after serum stimulation (Supplemental Figure 7D), expression of Fos in the *EWS/ATF1*-expressing tumor cell line was detected even under serum-free conditions, and it gradually increased after serum stimulation (Supplemental Figure 7E). Interestingly, whereas serum-stimulated MEFs revealed immediate phosphorylation of ERK1 and ERK2

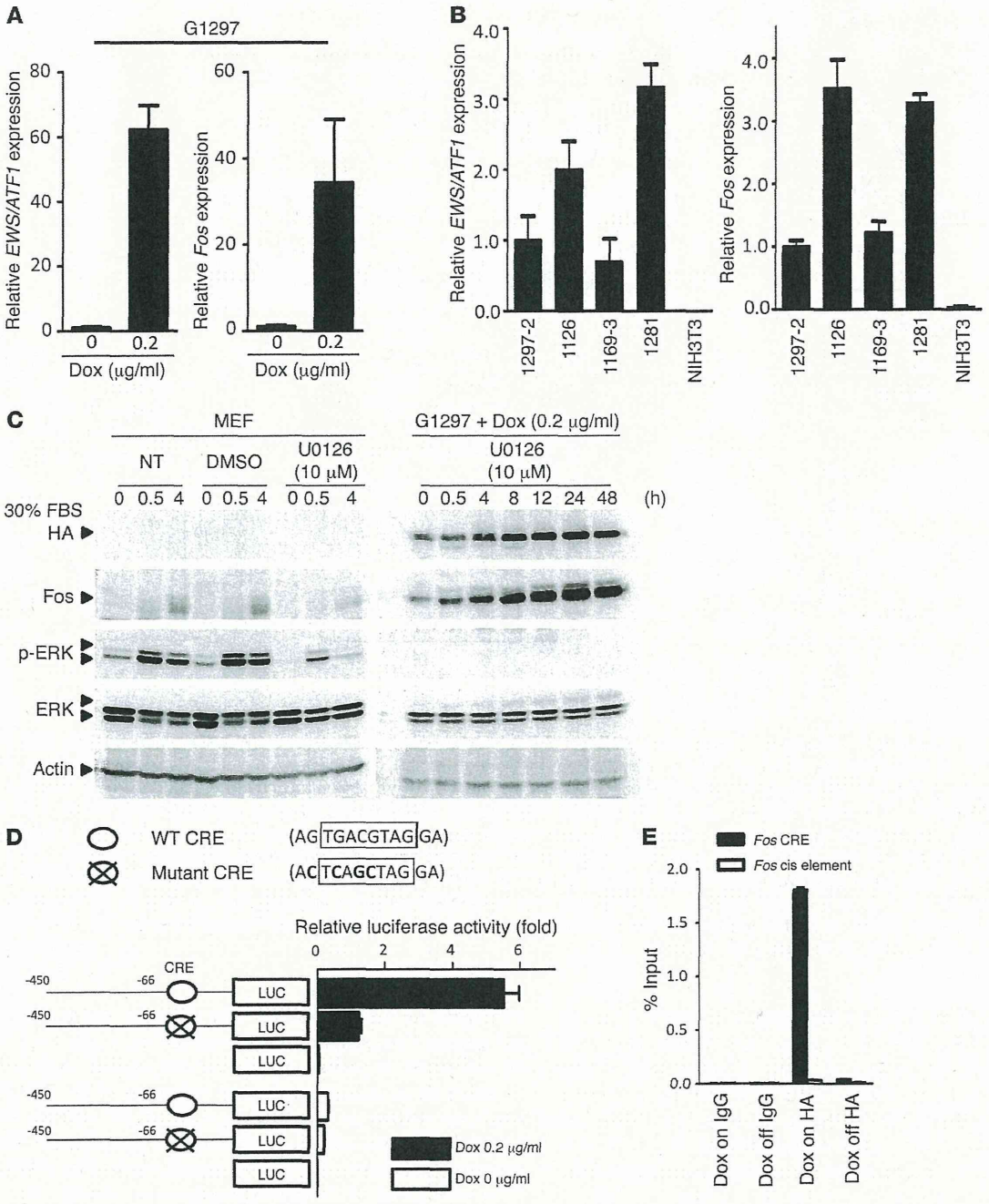

Figure 5

Fos is a direct target of EWS/ATF1. (**A**) Real-time RT-PCR analysis of G1297 cells revealed significant upregulation of both *EWS/ATF1* and *Fos* 3 hours after doxycycline exposure. (**B**) Relative expression of *EWS/ATF1* and *Fos* in 4 *EWS/ATF1*-induced tumors from 4 independent mice. NIH3T3 cells served as a control. Transcript levels were normalized to β-*actin*. Data are mean ± SD ($n = 3$). (**C**) Fos induction by *EWS/ATF1* was independent of the ERK pathway. Serum-starved MEFs and G1297 cells were stimulated with 30% FBS for the indicated times. Cells were also treated with 10 μM of the MEK inhibitor U0126. Whereas ERK1/2 inhibition by U0126 decreased Fos in MEFs, U0126 failed to suppress Fos expression in G1297 cells. NT, not treated. (**D**) Mouse *Fos* promoter–luciferase reporter constructs and pRL-SV40 vector (as an internal control) were cotransfected in G1297 cells treated with or without 0.2 μg/ml doxycycline. Luciferase activity of each construct was normalized to internal control activity. Data are mean ± SD ($n = 3$). (**E**) ChIP-PCR analysis was performed for the *Fos* promoter region containing CRE or the negative control cis element using HA-tag antibody or IgG as nonimmune immunoprecipitation, respectively. EWS/ATF1 was enriched at the CRE element of the *Fos* promoter in G1297 cells after treatment with 0.2 μg/ml doxycycline. Data (mean ± SD) were quantified by qRT-PCR and expressed as percent of input DNA.